VOL. 13, NO. 6, MARCH 2018 ISSN 1819-6608
ARPN Journal of Engineering and Applied Sciences

www.arpnjournals.com

A BIVARIATE VISCOSITY FUNCTION ON THE PERISTALTIC MOTION IN AN ASYMMETRIC CHANNEL

Mehdi Lachiheb
M. Lachiheb Faculty of Sciences, Taibah University, Kingdom of Saudi Arabia
E-Mail: lachiheb006@gmail.com

ABSTRACT

In this work, the movement of digestive juice in small intestine, food bolus through esophagus and the blood in arteries are addressed. Based on the characteristics of blood and digestive juices and the elements that affect them, a viscosity function adapted to an asymmetric channel is chosen to simulate some of the biological phenomena. A bivariate viscosity function reflects the natural phenomena where it is affected starting from the bottom and top walls as it occurs in the intestines and arteries. A peristaltic transport of Newtonian fluid is considered and the influence of the bivariate function in an asymmetric channel is studied. We were able to compute explicitly the pressure rise and the pressure gradient. Reflux, trapping, pumping and co pumping phenomena are studied. A graphical analysis of the effect of the viscosity variation is presented. Similar to the axisymmetric case, this work also illustrates that, the reflux limit and the free pumping do not depend on the viscosity parameter but the trapping limit, the pressure rise and the friction force on the walls, are influenced by the variation of this parameter.

Keywords: peristaltic motion, Newtonian fluid, small intestine, blood, trapping, reflux.

1. INTRODUCTION

Peristalsis is a progressive movement of contractions and relaxations that is typical of the membranes of elastic canals that move their contents forward or backward. Many biological phenomena correspond to the transfer of substances by the peristaltic movements such as the movement of digestive juice in small intestine, food bolus through esophagus and the blood in arteries, transport of urine through the ureters to the bladder and many others. Several factors such as viscosity, membranes shape, wave speed and type of fluid, directly affect the pressure, flow and particle velocity. Proper modeling requires the best representation of the factors that gives results that are significantly close to the natural state. Modeling peristaltic phenomenon has attracted considerable attention due of the variety of ways to represent them. This subject was started by Latham (1966) and Shapiro *et al.* (1969) with simple mathematical assumptions, constant viscosity, Newtonian fluid, symmetrical membrane given by a sine function and under a negligible Reynolds number and an infinitely long wavelength approximation. Then it is followed by a series of modifications in these assumptions that seem closer to reality. The symmetrical condition channel is replaced by asymmetric condition in Eytan and Elad (1999) and Mishra and Rao (2004). Shukla *et al*. (1980) studied the effect of the peripheral-layer viscosity and specified its interface shape independently of the fluid viscosities. Brasseur *et al*. (1987) used the mass conservation properties that were not satisfied in Shukla *et al.* (1980) and restudied the same problem and discussed the reflux and trapping phenomena. Elshehawey *et al*. (2004) split the interior channel area into three parts with three different viscosities. Muthu *et al.* (2001, 2008) considered the peristaltic transport in a cylindrical flexible tube with elastic or viscoelastic membrane conditions and that of micropolar fluid and studied the effect of wall properties. Srivastava *et al*. (1983a, b) treated the case of a symmetric variable viscosity that is dependent on the radial variable. El Misary *et al*. (2003) and Abd El Hakim *et al*. (2003) integrated an endoscope within the axis of the tube and studied its effects. Abd El Hakim *et al*. (2004) have chosen an exponential function viscosity dependent on a parameter and used the perturbation method whose variable is the same parameter for solve the problem. The integration of a viscosity function of one radial variable in an asymmetric channel is investigated by Hayat and Ali (2008). The incorrectness of their analysis was showed by Lachiheb (2016). Since the effect of top and bottom walls to viscosity is similar, an attentive selection of the viscosity function symmetrically affected by the two membranes, similar to the axisymmetric case, has been discussed. The latter again contradicted the physiological phenomena. Dharmendra (2011) considered a viscoelastic fluid in an inclined cylindrical tube for studying the flow of chyme in a small intestine. Recently, a magnetic field on peristaltic movement is considered by Rathod and Asha (2011). Rathod and Devindrappa (2013) used Adomian decomposition method to study the slip effect on peristaltic transport. The slip effects on magnetohydrodynamic peristaltic transport are studied by Hina *et al.* (2014). Without hypothesis about the wave form and tube length, Misra and Maiti (2012) developed a mathematical model representing the peristaltic motion of a rheological fluid. Hayet *et al.* (2014) considered a peristaltic motion in an inclined asymmetric channel with radial variable viscosity and thermal conductivity conditions. Abbasi *et al.* (2016) analyzed the peristaltic transport of non-Newtonian Maxwell fluid through a small radius tube. Kothandapani *et al*. (2016) studied the some problem with Johnson–Segalman fluid and tapered asymmetric channel conditions. Sher Akbar (2015a, b, c, d, e, f) also addressed many issues in this topic by adding or changing some hypotheses in the hope of solving some of biological questions. He used a Casson fluid with the existence of a magnetic field (Sher Akbar (2015a)). With

some boundary conditions, the magnetohydrodynamics of viscous fluids is the subject of Sher Akbar (2015b). He studied the entropy growth in the peristaltic transport (Sher Akbar (2015c, d)). Also, the peristaltic movement inan asymmetric channel and a non-uniform tube was used for certain applications such as by Sher Akbar (2015e) to follow the MHD nano "Eyring-Powell fluid" and by Sher Akbar (2015f) to analyze the effect of magnetic field on the flow and heat transfer of carbon nanotubes. The viscosity function used in previously mentioned works is either constant or a one radial variable function. However, a natural phenomenon of peristaltic movements shows that the viscosity decreases at the nearest point of the membrane. For instance, the movement of digestive juice in the small intestine is affected by a secretion of acids and water injected from the membrane (see Turvill and Farthing (1999); Costanzo (2009) and Lucas (2008)). During the blood motion in the arteries, the white blood cells and plasma are condensed in the center while the red blood cells are accumulated in the wall boundaries, resulting in a decrease in the value of the viscosity at the points closer to the wall (see Grobelnik 2008; Hayenes 1960; Bugliarello and Sevilla 1970; Gold Smith and Skalak 1975). This led Lachiheb (2014) to develop a bivariate viscosity function, and to study the effect of the new axial and radial function to the pumping flux, trapping and reflux phenomena in an axisymmetric conduit. Then, in each surface which admits an equation equal to that of the wall multiplied by a fixed number less than unity, the considered bivariate function remains invariant. Note that this selection provides a good modeling of the biological phenomena mentioned above. The goal of the current paper is to generalize the previous work (see Lachiheb (2014)) to asymmetric channel. We decided to present this work as follows. First, under some simplifying assumptions, a mathematical modeling of physical problems using Naiver Stokes is presented and an analytical expression for the pressure and its derivatives were determined after solving the Naiver Stokes equations. In the next section, we reported the most important theoretical and practical results obtained and a graphical discussion is presented. Finally, the concluding remarks are summarized in Section 4.

2. FORMULATION AND ANALYSIS

The fluid considered in our study is Newtonian and incompressible with bivariate viscosity that creeps through an asymmetric channel. The channel membrane is crossed by a stationary sinusoidal wave trains with a speed c. We assume $d_1 + d_2$ the channel width, $\bar{X}$ and $\bar{Y}$ the Cartesian coordinate,

$$\widehat{H_1}(\bar{X},\bar{t}) = d_1 + a_1 \cos\left((\frac{2\pi}{\lambda}(\bar{X} - c\bar{t})\right) \quad (1)$$

the geometry of the upper wall surface is (see Figure-1) and

$$\widehat{H_2}(\bar{X},\bar{t}) = -d_2 - a_2 \cos\left((\frac{2\pi}{\lambda}(\bar{X} - c\bar{t}) + \phi\right), \quad (2)$$

the equation of the upper wall, where λ is the wavelength, a_1 and a_2 are the waves amplitudes, $\bar{t}$ represents the time and ϕ $(0 \le \phi \le \pi)$ is the phase difference.

Also, the coefficients a_1, b_1, d_1, d_2 and ϕ satisfies the condition $a_1^2 + a_2^2 + 2a_1a_2cos(\phi) \le (d_1 + d_2)^2$.

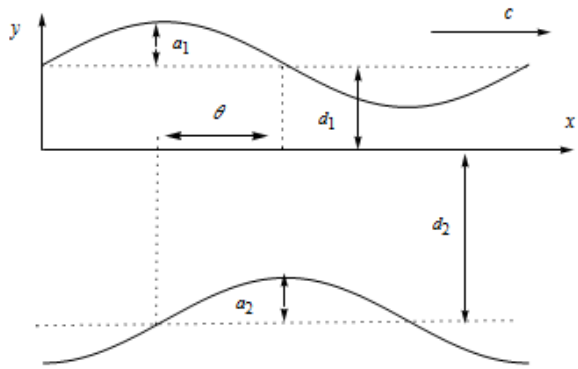

Figure-1. Asymmetric channel shape.

We note that the channel will be symmetric with waves out of phase if $\phi = 0$ and the waves are in phase if $\phi = \pi$.

We consider $(\bar{U},\bar{V})$ the components of velocity in the cartesian coordinate and $\bar{\Psi}$ the stream function. Since the flow is dependent to $\bar{t}$ in these coordinates then it is unsteady. A change of basis to another mobile which travel in the $\bar{x}$ direction with a constant speed c, make the movement is independent to $\bar{t}$ and the flow becomes steady. Let be $(\bar{x},\bar{y})$ the new coordinate, $(\bar{u},\bar{v})$ the components of velocity and $\bar{\psi}$ is the stream function in the moving basis. The coordinates transformations are given by:

$$\bar{x} = \bar{X} - c\bar{t} \qquad \bar{y} = \bar{Y} \quad (3)$$

$$\bar{v} = \bar{V} - c \qquad \bar{u} = \bar{U}$$
$$\bar{\psi} = \bar{\Psi} - \bar{y} + (\frac{\bar{H_1}+\bar{H_2}}{2}) \quad (4)$$

$$\bar{H_1}(\bar{x}) = d_1 + a_1 \cos(\frac{2\pi}{\lambda}\bar{x}) \quad (5)$$

$$\bar{H_2}(\bar{x}) = -d_2 - a_2 \cos(\frac{2\pi}{\lambda}\bar{x} + \phi) \quad (6)$$

Let be $\bar{\mu}$ the viscosity and $\bar{P}$ is the pressure function. In the moving basis, the continuity equation is

$$\frac{\partial\bar{u}}{\partial\bar{x}} + \frac{\partial\bar{v}}{\partial\bar{y}} = 0, \quad (7)$$

the Navier-Stokes equations are

$$\rho(\bar{u}\frac{\partial\bar{u}}{\partial\bar{x}} + \bar{v}\frac{\partial\bar{u}}{\partial\bar{y}}) = -\frac{\partial\bar{P}}{\partial\bar{x}} + 2\frac{\partial}{\partial\bar{x}}\left[\bar{\mu}(\bar{x},\bar{y})\frac{\partial\bar{u}}{\partial\bar{x}}\right] + \frac{\partial}{\partial\bar{y}}[\bar{\mu}(\bar{x},\bar{y})(\frac{\partial\bar{v}}{\partial\bar{x}} + \frac{\partial\bar{u}}{\partial\bar{y}})] \quad (8)$$

$$\rho(\bar{u}\frac{\partial\bar{v}}{\partial\bar{x}}+\bar{v}\frac{\partial\bar{v}}{\partial\bar{y}}) = -\frac{\partial\bar{P}}{\partial\bar{y}}+2\frac{\partial}{\partial\bar{y}}[\bar{\mu}(\bar{x},\bar{y})\frac{\partial\bar{v}}{\partial\bar{y}}]+\frac{\partial}{\partial\bar{x}}[\bar{\mu}(\bar{x},\bar{y})(\frac{\partial\bar{u}}{\partial\bar{y}}+\frac{\partial\bar{v}}{\partial\bar{x}})] \quad (9)$$

and the boundary conditions equations are

$$\bar{u}=-c \quad at \quad \bar{y}=\bar{H_1}, \quad or \quad \bar{y}=\bar{H_2} \quad (10)$$

$$\bar{v}=-c\frac{\partial\bar{H_1}(\bar{x})}{\partial\bar{x}} \quad at \quad \bar{y}=\bar{H_1} \quad and$$
$$\bar{v}=-c\frac{\partial\bar{H_2}(\bar{x})}{\partial\bar{x}} \quad at \quad \bar{y}=\bar{H_2} \quad (11)$$

The Reynolds number is defined by

$$Re=\frac{cd_1\rho}{\mu_0} \quad (12)$$

where $\mu_0=\bar{\mu}(\bar{x},\frac{\bar{H_1}+\bar{H_2}}{2})$ the viscosity at $\frac{\bar{H_1}+\bar{H_2}}{2}$, assumed to be constant, and the wave number by

$$\delta=\frac{d_1}{\lambda} \quad (13)$$

In the following we present the non-dimensional variables:

$$y=\frac{\bar{y}}{d_1} \quad x=\frac{\bar{x}}{\lambda}, \quad u=\frac{\bar{u}}{c}, \quad v=\frac{\bar{v}}{\delta c},$$
$$P=\frac{d_1^2\bar{P}}{c\lambda\mu_0}, \quad \mu=\frac{\bar{\mu}}{\mu_0}, \quad t=\frac{c\bar{t}}{\lambda}, \quad H_1=\frac{\bar{H_1}}{d_1},$$
$$H_2=\frac{\bar{H_2}}{d_1}, a=\frac{a_1}{d_1}, d=\frac{d_2}{d_1}, \quad b=\frac{b_1}{d_1},$$
$$\psi=\frac{\bar{\psi}}{cd_1}, \quad \Psi=\frac{\bar{\Psi}}{cd_1}. \quad (14)$$

If we replace the last quantities in the equations (7, 8, 9, 10) we obtain

$$\frac{\partial u}{\partial x}+\frac{\partial v}{\partial y}=0 \quad (15)$$

$$Re\delta^3\left(u\frac{\partial v}{\partial x}+v\frac{\partial v}{\partial y}\right)=-\frac{\partial P}{\partial y}+2\delta^2\frac{\partial}{\partial y}[\mu(x,y)\frac{\partial v}{\partial y}]+\frac{\partial}{\partial y}[\mu(y)(\delta^2\frac{\partial v}{\partial x}+\frac{\partial u}{\partial y})] \quad (16)$$

$$Re\delta^3\left(u\frac{\partial v}{\partial x}+v\frac{\partial v}{\partial y}\right)=-\frac{\partial P}{\partial y}+2\delta^2\frac{\partial}{\partial y}[\mu(x,y)\frac{\partial v}{\partial y}]+\delta^2\frac{\partial}{\partial x}[\mu(x,y)(\frac{\partial u}{\partial y}+\delta^2\frac{\partial v}{\partial x})] \quad (17)$$

$$u=-1 \quad at \quad y=H_1=1+acos(2\pi x), \quad or$$
$$y=H_2=-d-bcos(2\pi x+\phi) \quad (18)$$

$$v=-\frac{\partial H_1(x)}{\partial x} \quad at \quad y=H_1 \quad and$$
$$v=-\frac{\partial H_2(x)}{\partial x} \quad at \quad y=H_2 \quad (19)$$

If we use the the negligible Reynolds number and the long wavelength approximation we obtain:

$$\frac{\partial u}{\partial x}+\frac{\partial v}{\partial y}=0 \quad (20)$$

$$\frac{\partial P}{\partial y}=0 \quad (21)$$

$$\frac{\partial P}{\partial x}=\frac{\partial}{\partial y}\left(\mu(x,y)\frac{\partial u}{\partial y}\right) \quad (22)$$

In the fixed and moving coordinate system, the instantaneous volume flow rate are defined by:

$$\hat{Q}=\int_{\bar{H_2}}^{\bar{H_1}}\bar{U}\,d\bar{Y} \quad (23)$$

$$\bar{q}=\int_{\bar{H_2}}^{\bar{H_1}}\bar{u}\,d\bar{y} \quad (24)$$

From equations (3, 4, 5, 6) and (23, 24), we obtain:

$$\hat{Q}=\bar{q}+c\widehat{H_1}-c\widehat{H_2} \quad (25)$$

Also, we find

$$Q=\frac{\bar{q}}{d_1c}=\int_{H_2}^{H_1}u\,dy \quad (26)$$

The time-mean flow over a period $T=\frac{\lambda}{c}$ at a fixed $\bar{X}$-position is defined as

$$\bar{Q}=\frac{1}{T}\int_0^T\hat{Q}\,d\bar{t}=\bar{q}+cd_1+cd_2 \quad (27)$$

The dimensionless time-mean flow is

$$\Theta=\frac{\bar{Q}}{cd_1}=Q+1+d \quad (28)$$

Since the pressure is constant along y variable and from equation (22) it follows that $\mu(x,y)\frac{\partial u}{\partial y}=y\frac{\partial P}{\partial x}+c_1(x)$, where $c_1(x)$ is a function dependent on x.

Then $u(x,y)=I_1(x,y)\frac{\partial P}{\partial x}+c_1(x)I_0(x,y)+c_2(x)$, where $I_1(x,y)=\int_{H_2(x)}^{y}\frac{t}{\mu(x,t)}dt$ and $I_0(x,y)=\int_{H_2}^{y}\frac{1}{\mu(x,t)}dt$. We used the second part of (18), we obtain $c_2(z)=-1$, and the first part of (18), we obtain $c_1(x)=-\frac{\partial P}{\partial x}\frac{I_1(x,H_1)}{I_0(x,H_1)}$

$$u(x,y)=\frac{\partial P}{\partial x}[I_1(x,y)-\frac{I_1(x,H_1)}{I_0(x,H_1)}I_0(x,y)]-1 \quad (29)$$

and

$$\frac{\partial\psi}{\partial y}=\frac{\partial P}{\partial x}[I_1(x,y)-\frac{I_1(x,H_1)}{I_0(x,H_1)}I_0(x,y)]-1 \quad (30)$$

Replacing the velocity component u by the right hand side of (29) in (26) and using $\int_{H_2}^{y}(\int_{H_2}^{z}\frac{t}{\mu(x,t)dt})dz=$

$y\int_{H_2}^{y}\frac{t}{\mu(x,t)}dt-\int_{H_2}^{y}\frac{t^2}{\mu(x,t)}dt$ and $\int_{H_2}^{y}(\int_{H_2}^{z}\frac{1}{\mu(x,t)dt})dz = y\int_{H_2}^{y}\frac{1}{\mu(x,t)}dt-\int_{H_2}^{y}\frac{t}{\mu(x,t)}dt$, we find that

$$Q=-\frac{\partial P}{\partial x}[I_2(x,H_1)-\frac{(I_1(x,H_1))^2}{I_0(x,H_1)}]-(H_1-H_2) \tag{31}$$

and thus

$$\frac{\partial P}{\partial z}=-\frac{Q+H_1-H_2}{I_2(x,H_1)-\frac{(I_1(x,H_1))^2}{I_0(x,H_1)}} \tag{32}$$

and where

$$I_2(x,y)=\int_{H_2(x)}^{y}\frac{t^2}{\mu(x,t)}dt$$

since $\psi=-\frac{Q}{2}$ at $r=H_2$, it follows that

$$\psi=-\frac{Q+H_1-H_2}{I_2(x,H_1)-\frac{(I_1(x,H_1))^2}{I_0(x,H_1)}}[yI_1(x,y)-I_2(x,y)-\frac{I_1(x,H_1)}{I_0(x,H_1)}(yI_0(x,y)-I_1(x,y))]-(y-H_2)-\frac{Q}{2} \tag{33}$$

In previously worked with axisymmetric conduit (Lachiheb (2014)), we considered the viscosity to be a bivariate function in the following form:

$$\mu(x,y)=f(\frac{y}{H(x)}) \tag{34}$$

where $f(r)=e^{-\alpha r}$.

This choice is motivated by the following physiological phenomena. First the chyme viscosity is affected by a secretion of plenty of liquids. The latter consists mainly of water and acids and is injected into the lumen of intestine from the wall (Turvill and Farthing 1999; Costanzo 2009; Lucas 2008). Second, during the blood motion in the arteries, the white blood cells and plasma are condensed in the center while the red blood cells are accumulated in the wall boundaries, resulting in a decrease in the value of the viscosity at the points more closer to the wall (Grobelnik 2008; Hayenes 1960; Bugliarello and Sevilla 1970; Gold Smith and Skalak 1975). The biological observations can be interpreted by the invariance of the viscosity function on each proportional membrane surfaces. Which again contradicts the assumptions on the viscosity given by Shapiro *et al.* (1969); Mishra and Rao (2004); Srivastava *et al*. (1983a, b) and Hayat and Ali (2008) which implies that the invariance of viscosity along lines parallel to the axis. Like in the symmetric situation (Lachiheb (2014)), the viscosity function is subject to the influence of two different walls at the top and the bottom, resulting in a constant viscosity at the midpoints between the two walls. Thus, the stream-lines of viscosity in each half of the channel is influenced by the form of the outer wall and the shape of midpoints. To achieve the most important of these observations we define the following function

$$\mu(x,y)=f(\frac{y-\frac{(H_1+H_2)}{2}}{\frac{H_1-H_2}{2}}) \quad if \quad y\geq\frac{(H_1+H_2)}{2}$$
$$\mu(x,y)=f(\frac{\frac{(H_1+H_2)}{2}-y}{\frac{H_1-H_2}{2}}) \quad if \quad y\leq\frac{(H_1+H_2)}{2} \tag{35}$$

Note that in each half part of the channel the viscosity rest invariable throughout the distant points at the midpoints by a distance equal to $\frac{H_1-H_2}{2}$ product by a constant less than unity. Figures 2 and 3 are made to see the invariant viscosity lines in two cases $\phi=\pi/3$ and $\phi=0$ (axisymmetric case).

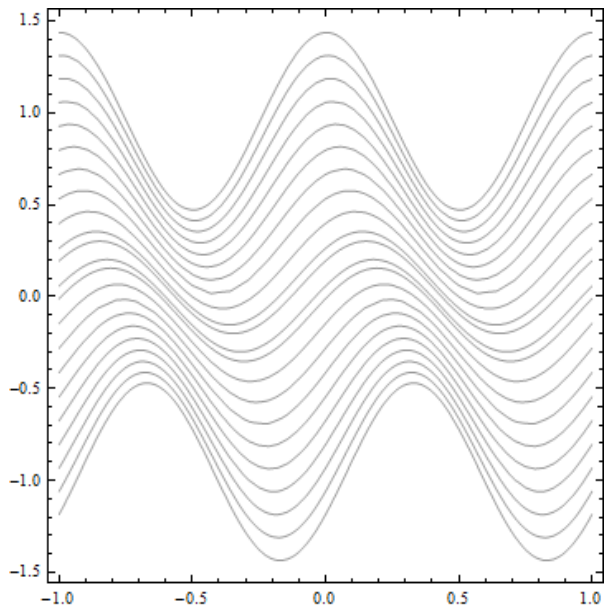

Figure-2. The invariant viscosity lines ($a=0.5$, $b=0.5$, $d=1$ and $\phi=\pi/3$).

Also, this selection provides a good modeling of the biological phenomena mentioned above. Moreover, many positive and negative real numbers are considered for the viscosity parameter for representing a decreasing and increasing viscosity.

Replacing equation (35) in $I_0(x,y)$, $I_1(x,y)$ and $I_2(x,y)$ we obtain

$$\frac{\partial P}{\partial z}=-4\alpha^3\frac{Q+H_1-H_2}{\beta(H_1-H_2)^3} \tag{36}$$

where

$$\beta=(-2+(2+(-2+\alpha)\alpha)e^{\alpha})$$

and

$$\psi = \frac{(H_1-H_2+Q)}{2\beta(H_1-H_2)}\left(e^{-\frac{\alpha(H_1+H_2-2y)}{H_1-H_2}}((\alpha+2)H_1 + (\alpha-2)H_2 - 2\alpha y) - e^{\alpha}((\alpha(2\alpha-3)+2)H_1 + (\alpha-2)H_2 - 2(\alpha-1)\alpha y)\right) + H_1 + \frac{Q}{2} - y \quad if\ y \geq \frac{(H_1+H_2)}{2}$$
$$\psi = \frac{(H_1-H_2+Q)}{2\beta(H_1-H_2)}\left(e^{\frac{\alpha(H_1+H_2-2y)}{H_1-H_2}}((\alpha-2)H_1 (\alpha+2)H_2 - 2\alpha y) - e^{\alpha}((\alpha-2)H_1 + (\alpha(2\alpha-3)+2)H_2 - 2(\alpha-1)\alpha y)\right) + H_2 - \frac{Q}{2} - y \quad if\ y \leq \frac{(H_1+H_2)}{2} \tag{37}$$

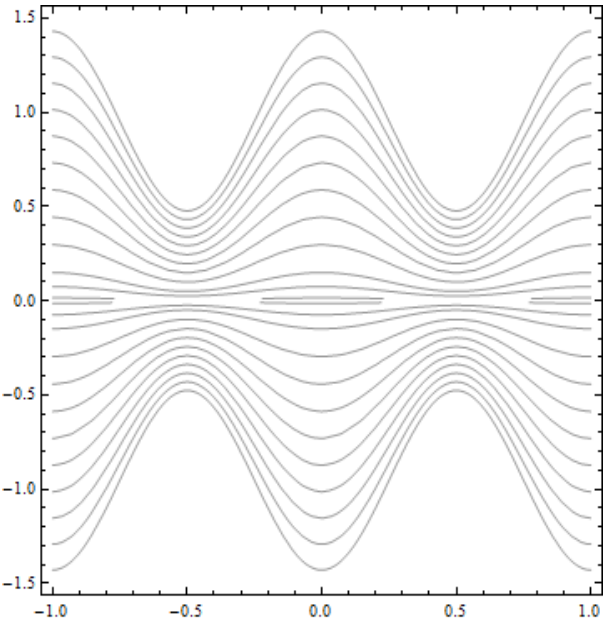

Figure-3. The invariant viscosity lines ($a = 0.5$, $b = 0.5$, $d = 1$ and $\phi = 0$).

In non-dimensional forms, the pressure rise ΔP_λ and friction force F_λ are defined by

$$\Delta P_\lambda = \int_0^1 \frac{\partial P}{\partial z} dz \tag{38}$$

$$F_\lambda^u = \int_0^1 H_1^2 \left(-\frac{\partial P}{\partial z}\right) dz \tag{39}$$

$$F_\lambda^l = \int_0^1 H_2^2 \left(-\frac{\partial P}{\partial z}\right) dz \tag{40}$$

Replacing equation (36) in (38), (39) and (40) we get

$$\Delta P_\lambda = -\frac{2\alpha^3}{\beta}(\Theta - (1+d)) \frac{2(1+d)^2+(a^2+b^2+2ab\cos(\phi))}{((1+d)^2-(a^2+b^2+2ab\cos(\phi)))^{\frac{5}{2}}} - \frac{4\alpha^3}{\beta}\frac{(1+d)}{((1+d)^2-(a^2+b^2+2ab\cos(\phi)))^{\frac{3}{2}}} \tag{41}$$

and this is rewritten in the form

$$\Theta = -\frac{\beta\Delta P_\lambda}{2\alpha^3}\frac{((1+d)^2-(a^2+b^2+2ab\cos(\phi)))^{\frac{5}{2}}}{(2(1+d)^2+(a^2+b^2+2ab\cos(\phi)))} + \frac{3(1+d)(a^2+b^2+2ab\cos(\phi))}{(2(1+d)^2+(a^2+b^2+2ab\cos(\phi)))} \tag{42}$$

$$F_\lambda^u = \frac{4\alpha^3}{\beta}\Big[\frac{(\Theta-(d+1))}{2((d+1)^2-\beta_2)^{\frac{5}{2}}}(2a^4 + a^2(\frac{b^2}{2} + (d-4)d - 4) + \frac{1}{2}ab(4(2a^2-3d-2)\cos(\phi) + 3ab\cos(2\phi)) + b^2 + 2(d+1)^2) - \frac{1}{\beta_2^2((d+1)^2-\beta_2)^{\frac{3}{2}}}(a^2(d+1)^3\beta_1 - a^2(d+1)^2\beta_1\sqrt{(d+1)^2-\beta_2} - (d+1)\beta_2 \big((2a^2+1)(a+b\cos(\phi))^2 - (a^2-1)b^2 sin^2(\phi)\big) - a(a+b\cos(\phi))^4\sqrt{(d+1)^2-\beta_2} + 2\beta_2^2(a+b\cos(\phi)) - ab^4\sin^4(\phi)\sqrt{(d+1)^2-\beta_2})\Big] \tag{43}$$

$$F_\lambda^l = \frac{4\alpha^3}{\beta}\Big[\frac{(\Theta-(d+1))}{4((d+1)^2-\beta_2)^{\frac{5}{2}}}(b^2(a^2 - 8d(d+1) + 2) + 2d^2(a^2 + 2(d+1)^2) + ab(3ab\cos(2\phi) + 4(2b^2 - d(2d+3))\cos(\phi)) + 4b^4) + \frac{1}{\beta_2^2((d+1)^2-\beta_2)^{\frac{3}{2}}}(\frac{1}{2}(d+1)\beta_2(2d^2(a^2+b^2) + b^2(a^2+4b^2) + ab(3ab\cos(2\phi) + 4(2b^2+d^2)\cos(\phi))) - b^2(d+1)^3\beta_3 - b^2(d+1)^2\sqrt{(d+1)^2-\beta_2}(-a\sin(\phi) + a\cos(\phi) + b)(a(\sin(\phi)+\cos(\phi)) + b) - b\beta_2(a^2b\cos(2\phi)(\sqrt{(d+1)^2-\beta_2} + 2d) + 2a\cos(\phi)(b^2(\sqrt{(d+1)^2-\beta_2} + 3d) + a^2d) + b^3(\sqrt{(d+1)^2-\beta_2} + 2d) + 4a^2bd))\Big] \tag{44}$$

where $\beta_1 = a^2 + 2ab\cos(\phi) + b^2\cos(2\phi)$, $\beta_2 = a^2 + 2ab\cos(\phi) + b^2$ and $\beta_3 = a^2\cos(2\phi) + 2ab\cos(\phi) + b^2$.

If α closes to zero, we have the results reported by Mishra and Rao (2004).

$$\psi = \frac{(H_2^3-3H_1H_2^2)\left(H_1+\frac{Q}{2}\right)-(H_1^3-3H_1^2H_2)\left(H_2-\frac{Q}{2}\right)}{(H_2-H_1)^3} + \frac{(H_1-H_2+Q)(-3y^2(H_1+H_2)+6H_1H_2y+2y^3)}{(H_2-H_1)^3} - y \tag{45}$$

$$\Delta P_\lambda = -6(\Theta - (1+d)) \frac{2(1+d)^2+(a^2+b^2+2ab\cos(\phi))}{((1+d^2)-(a^2+b^2+2ab\cos(\phi)))^{\frac{5}{2}}} - 12\frac{(1+d)}{((1+d^2)-(a^2+b^2+2ab\cos(\phi)))^{\frac{3}{2}}} \tag{46}$$

and if $H_1 = -H_2$ (i.e. $\phi = 0, b = a, d = 1$) , we obtain

$$\psi = \frac{(2H_1+Q)}{4((\alpha-2)\alpha+2)e^{\alpha}-2)H_1}\left(e^{-\frac{\alpha y}{H_1}}(2\alpha y + 4H_1) - e^{\alpha}(-(\alpha-2)H_1 + (\alpha(2\alpha-3)+2)H_1 + 2(\alpha-1)\alpha y)\right) + H_1 + \frac{Q}{2} + y, \tag{47}$$

$$\Delta P_\lambda = -\frac{2\alpha^3}{\beta}(\Theta - 2)\frac{8+4a^2}{(4-4a^2)^{\frac{5}{2}}} - \frac{4\alpha^3}{\beta}\frac{2}{(4-4a^2)^{\frac{3}{2}}} \quad (48)$$

And

$$F_\lambda^u = F_\lambda^l = \frac{4\alpha^3}{\beta}\frac{\Theta-\sqrt{1-a^2}-2}{4\sqrt{1-a^2}} \quad (49)$$

3. DISCUSSION OF THE RESULTS

3. 1. Pumping characteristics

The value of the pressure rise when the flow rate is zero is called the maximum pressure rise ΔP_{max}. It is the boundary where the peristaltic functions as a pump. Also, if the pressure rise is equal to zero ($\Delta P = 0$), we obtain the maximum flow rate Θ_{max}. Then the maximum flow rate corresponds to the free pumping. ΔP_{max} and Θ_{max} are determined by

$$\Delta P_{max} = \frac{6\alpha^3}{\beta}\frac{(1+d)(a^2+b^2+2ab\cos(\phi))}{((1+d)^2-(a^2+b^2+2ab\cos(\phi)))^{\frac{5}{2}}} \quad (50)$$

$$\Theta_{max} = \frac{3(1+d)(a^2+b^2+2ab\cos(\phi))}{2(1+d)^2+(a^2+b^2+2ab\cos(\phi))} \quad (51)$$

The flux is negative when $\Delta P > \Delta P_{max}$ and we obtain the copumping region $\Theta > \Theta_{max}$ if $\Delta P < 0$ when the pressure assists the flow.

It has been noticed that the free pumping is independent to the parameter α but the maximum pressure rise is the product of that of constant viscosity by a factor $\frac{\alpha^3}{3\beta}$ which is less than 1 if α positive and is greater than 1 elsewhere.

Figures 4-6 present the pressure rise and friction forces at the lower and upper walls versus flow rate for different viscosity functions and four values of ϕ ($\phi = 0$, $\phi = \pi/4$, $\phi = \pi/2$, $\phi = \pi$) at $a = 0.7$, $b = 1.2$, and $d = 2$. For the reason that the considered viscosity functions by Srivastava *et al.* (1983a,b) ; Mishra and Rao (2004) and Hayet and Ali (2008) is $1 - \alpha r$ the linear approximation of $e^{-\alpha r}$ where $\alpha = 0$ or $\alpha = 0.1$, Figure-4 presents the variation of the pressure rise on the walls versus flow rate according to the different viscosities mentioned above. First, it is observed that the pressure rise curves for the bivariate viscosity ($\mu(x,y) = e^{-\alpha\frac{y-\sigma}{\tau}}$, $\sigma = \frac{H_1+H_2}{2}$ and $\tau = \frac{H_1-H_2}{2}$) lie under that for constant viscosity in the pumping region for all values of phase difference ϕ, and the situation is quite opposite in copumping region but Θ_{max} is independent of α. Second, the pressure rise curves for the bivariate viscosity lie under that for the one variable viscosity as reported by Hayat and Ali (2008) and Lachiheb (2014) in the co pumping region for all values of the phase difference ϕ, while in the pumping region, the situation is quite opposite for ϕ close to π and the first curve lie under that the second but they are almost identical for ϕ close to 0. These observations are clearly obtained from Figure-4. Similar to the last graphics, Figures 5 and 6 are made to see the influence of variable viscosity on the frictional forces at the lower and upper walls respectively. We note that the norm of frictional force on the upper wall for the bivariate viscosity is less than that for constant viscosity for all values of ϕ and is greater than that for one variable viscosity function for all values of ϕ closer to π. For ϕ closer to 0, the curve of frictional force on the upper wall for radial variability of viscosity lie under that for the bivariate viscosity. For frictional force on the lower wall, it is noted that the relationship between the three curves is similar to that achieved by the curves of Figure-7.

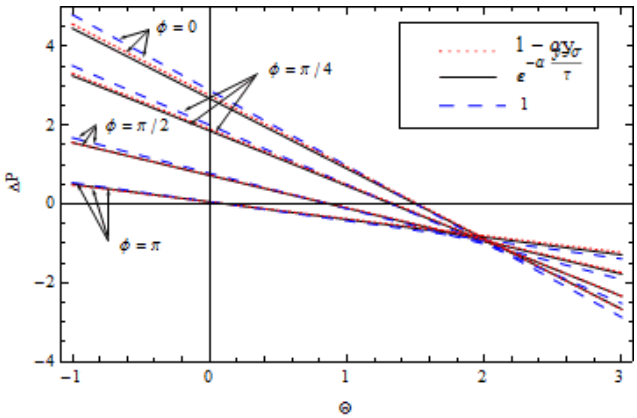

Figure-4. The pressure rise ΔP versus the volume flow rate θ with $a = 0.7$, $b = 1.2$ and $d = 2$.

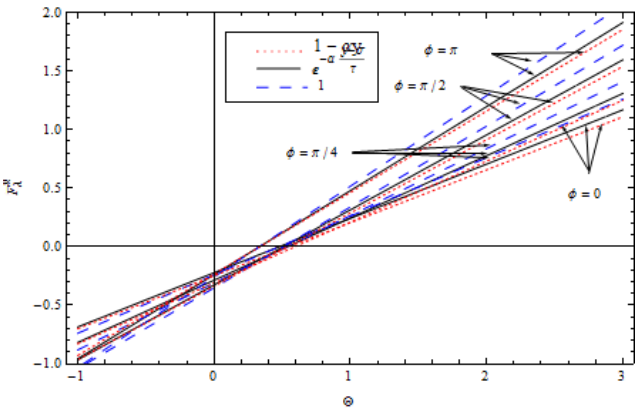

Figure-5. The friction force on the upper wall F_λ^u versus the volume flow rate θ with with $a = 0.7$, $b = 1.2$ and $d = 2$.

VOL. 13, NO. 6, MARCH 2018 ISSN 1819-6608
ARPN Journal of Engineering and Applied Sciences

www.arpnjournals.com

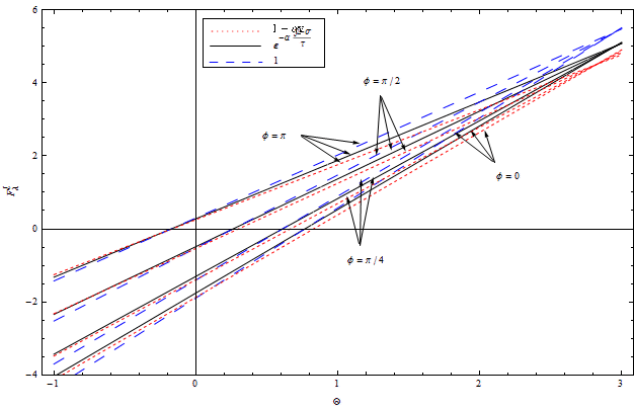

Figure-6. The friction force on the lower wall F_λ^l versus the volume flow rate θ witha $= 0.7$, $b = 1.2$ and d $= 2$.

The change in position of the two curves of the friction force on the upper wall (resp. lower wall) with different viscosity functions is clearly seen in Figure-8 (resp. Figure-9). The variation of ΔP, F_λ^u and F_λ^l with Θ at $a = 0.7$, $b = 1.2$, $d = 2$ and $\phi = \frac{\pi}{4}$ for different values of viscosity parameter α ($\alpha = -0.2$, $\alpha = -0.1$, $\alpha = 0.1$, $\alpha = 0.2$, $\alpha = 0.5$, $\alpha = 1$) is shown in Figures 10-12. It is observed that the pressure rise and the frictional forces on upper and lower walls decrease with increasing α.

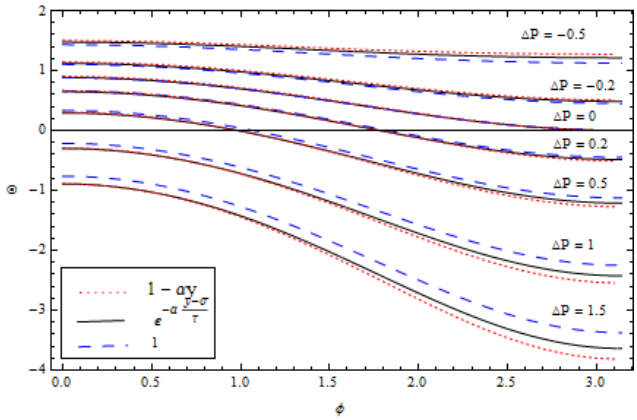

Figure-7. The volume flow rate θ versus the phase difference ϕ with $a = 0.7$, $b = 1.2$ and $d = 2$.

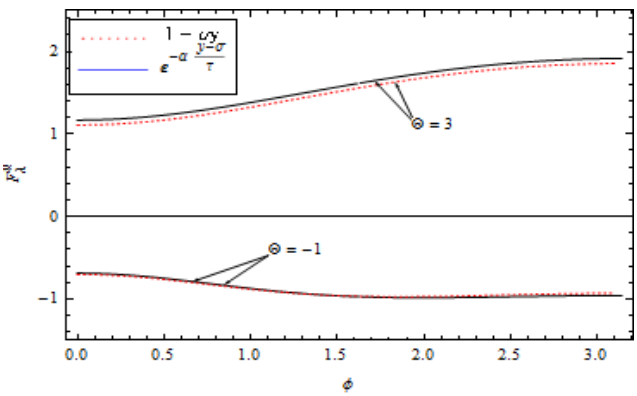

Figure-8. The friction force on the upper wall F_λ^u versus the phase difference ϕ with$a = 0.7$, $b = 1.2$ and $d = 2$.

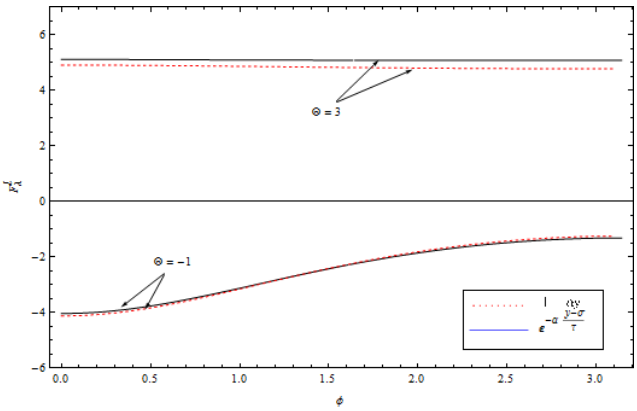

Figure-9. The friction force on the lower wall F_λ^l versus the phase difference ϕ witha $= 0.7$, b $= 1.2$ and d $= 2$.

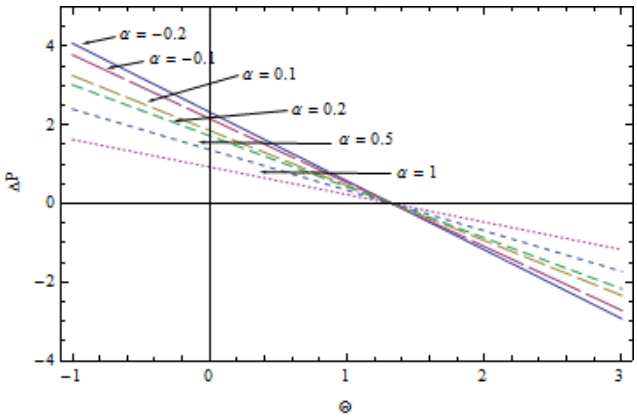

Figure-10. The pressure rise ΔP versus the volume flow rate θ at $a = 0.7$, $b = 1.2$, $d = 2$ and $\phi = \pi/4$ with increasing viscosity.

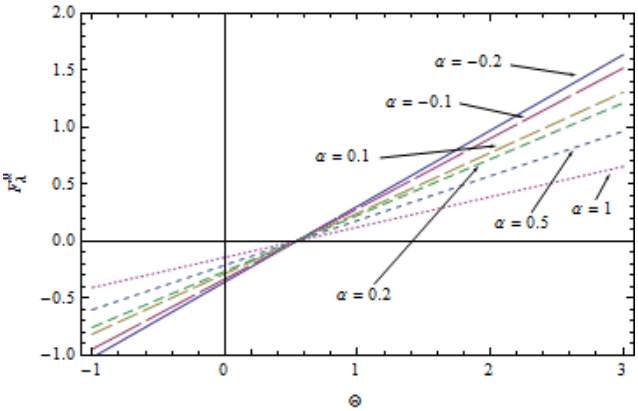

Figure-11. The friction force on the upper wall F_λ^u versus the volume flow rate θ at $a = 0.7$, $b = 1.2$, $d = 2$ and $\phi = \pi/4$ with increasing viscosity .

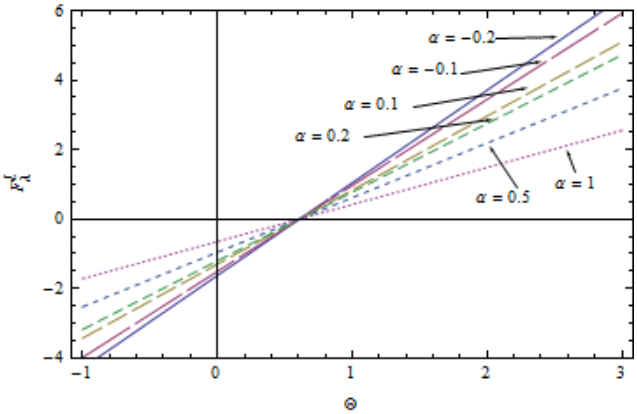

Figure-12. F_λ^l versus the volume flow rate θ at $a = 0.7$, $b = 1.2$, $d = 2$ and $\phi = \pi/4$ with increasing viscosity .

The pressure rise and frictional forces at the lower and upper walls versus flow rate for different viscosity functions, four values of a ($a = 0.2$, $a = 0.4$, $a = 0.6$, $a = 0.8$), four values of b ($b = 0.3$,$b = 0.5$, $b = 0.8$, $b = 1.2$) and four values of d ($d = 1.8$, $d = 1.9$, $d = 2$, $d = 2.1$) are plotted in Figures 13-15, figures 16-18 and Figures 19-21 respectively. For each parameter, the position of the three curves defined by different viscosity functions in each figure is similar to that of the Figures 4, 6, 7 respectively.

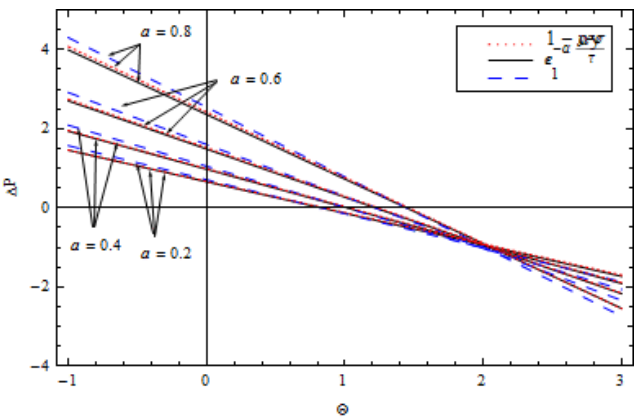

Figure-13. The pressure rise ΔP versus the volume flow rate θ with $b = 1.2$ and $d = 2$ and $\phi = \pi/4$.

Indeed, the norm of the pressure rise and the friction forces for the bivariate viscosity is less than that for constant viscosity respectively for all values of ϕ, a, b and d, while the curve of the frictional forces and the pressure rise for the bivariate viscosity lie under that for one variable viscosity function respectively, for most of values of ϕ, a, b and d.

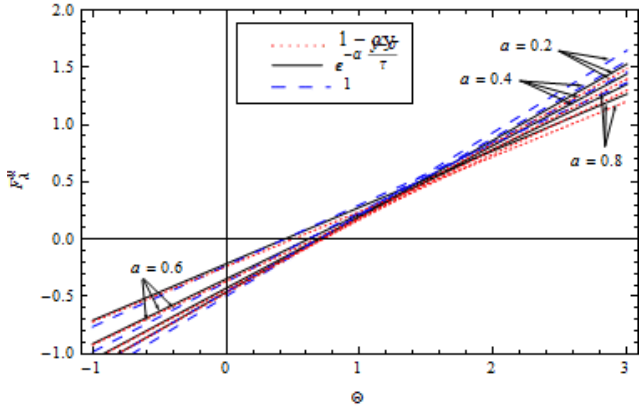

Figure-14. F_λ^u versus the volume flow rate θ with $b = 1.2$ and $d = 2$ and $= \pi/4$.

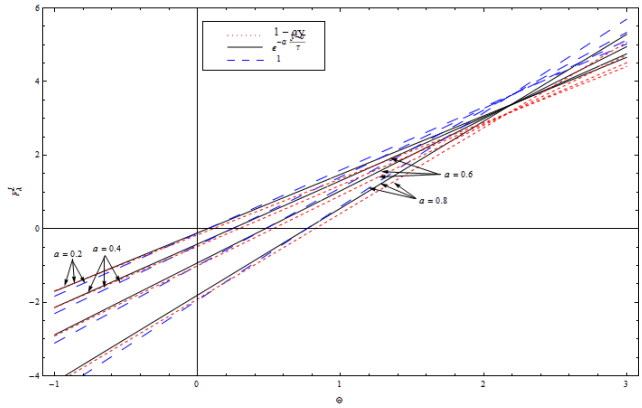

Figure-15. The friction force on the lower wall F_λ^l versus the volume flow rate θ with $b = 1.2$ and $d = 2$ and$= \pi/4$.

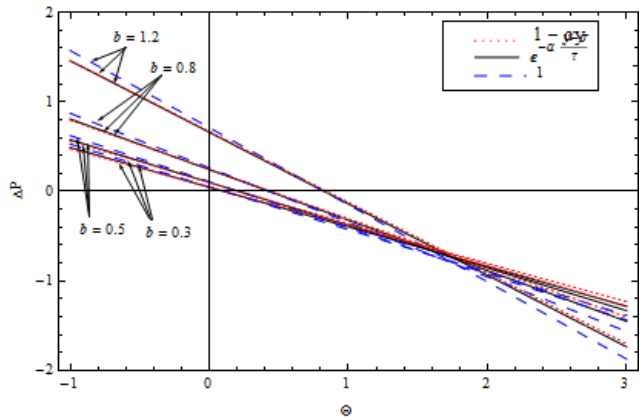

Figure-16. The pressure rise ΔP versus the volume flow rate θ with $a = 0.2$ and $d = 2$ and $= \pi/4$.

The situation is quite opposite in the pumping region and the region where the friction forces have a direction opposite to that of the wave velocity for some values of ϕ, a, b and d such that ϕ close to π or a to 0.2 or b to 0.3 or d to 2. In these latter cases the two curves for pressure rise or friction forces with different viscosity functions are almost identical.

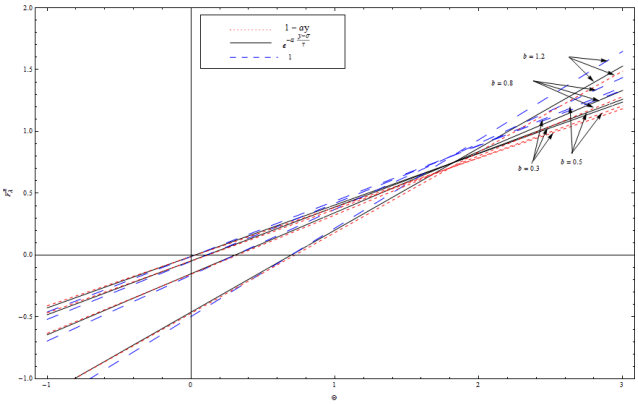

Figure-17. F_λ^u versus the volume flow rate θ with $a = 0.2$ and $d = 2$ and $= \pi/4$.

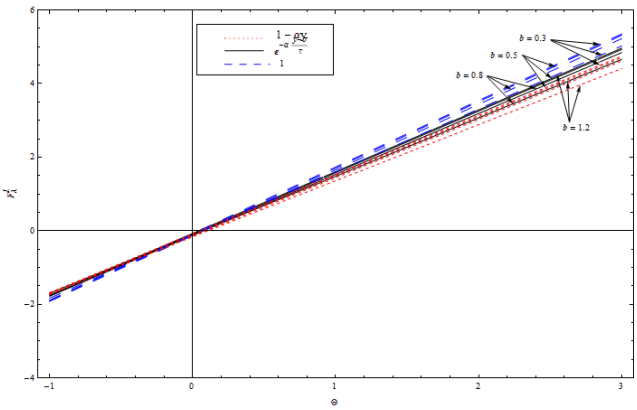

Figure-18. The friction force on the lower wall F_λ^l versus the volume flow rate θ with $a = 0.2$ and $d = 2$ and $\phi = \pi/4$.

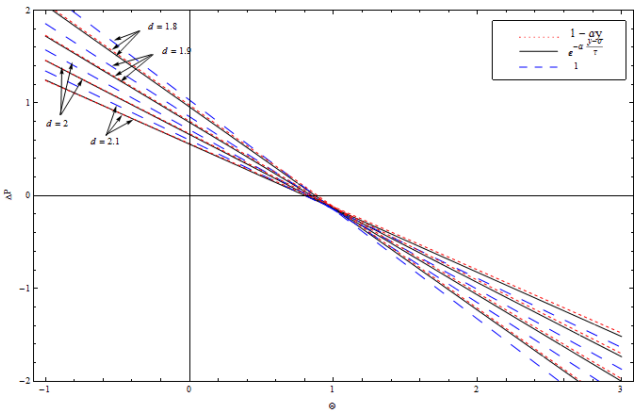

Figure-19. The pressure rise ΔP versus the volume flow rate θ with $a = 0.2$ and $b = 1.2$ and $= \pi/4$.

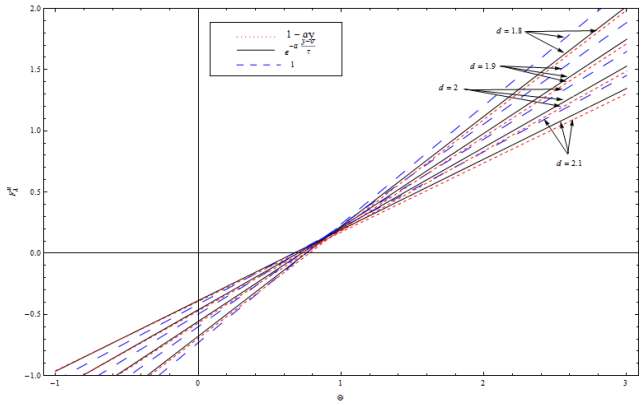

Figure-20. The friction force F_λ^u versus the volume flow rate θ with $a = 0.2$ and $b = 1.2$ and $\phi = \pi/4$.

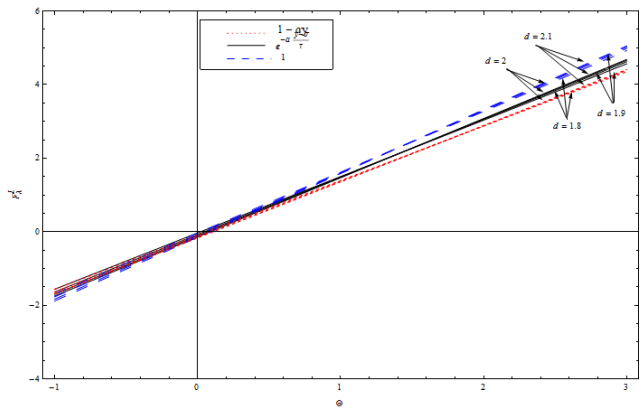

Figure-21. The friction force F_λ^l versus the volume flow rate θ with $a = 0.2$ and $b = 1.2$ and $\phi = \pi/4$.

3.2. Trapping limit

A region of closed streamlines is formed for certain combination of Θ and ϕ. If the mean speed of this region is equal to c, this phenomenon is called trapping. This phenomenon can appear in peristaltic motion when the membrane is sufficiently occluded. The trapping limit is defined by all values of Θ where $\psi = 0$ at some y different then $\frac{H_1+H_2}{2}$. The power series expression of ψ in terms of $r = y - \frac{H_1+H_2}{2}$, shows that there exists a center streamline $\psi = 0$ at $y = \frac{H_1+H_2}{2}$ and if the following equation is satisfy

$$1 - \frac{(\alpha(3+(-1+\alpha)e^{\alpha})(\frac{(H_1-H_2)}{2}+\theta-(1+d)))}{(\frac{H_1-H_2}{2}(-2+(2+(-2+\alpha)\alpha)e^{\alpha})} = 0 \qquad (52)$$

for some flow rate Θ. Then the flow-rate Θ for which trapping may occur lies between two extremes as given below

$$\Theta^- = -\sqrt{a^2+b^2+2ab\cos\phi} + \frac{(-2+(2+(-2+\alpha)\alpha)e^{\alpha})(1+d+\sqrt{a^2+b^2+2ab\cos\phi})}{\alpha+(-1+\alpha)\alpha e^{\alpha}} \qquad (53)$$

and

$$\Theta^{+} = \sqrt{a^2+b^2+2ab\cos\phi} + \frac{(-2+(2+(-2+\alpha)\alpha)e^{\alpha})(1+d-\sqrt{a^2+b^2+2ab\cos\phi})}{\alpha+(-1+\alpha)\alpha e^{\alpha}} \quad (54)$$

If $H_2 = -H_2$ then $a = b$, $d = 1$ and $\phi = 0$, we have the range for Newtonian fluid in axisymmetric given by

$$\Theta^{-} = -2a + \frac{(-2+(2+(-2+\alpha)\alpha)e^{\alpha})(2+2a)}{\alpha+(-1+\alpha)\alpha e^{\alpha}} \quad (55)$$

and

$$\Theta^{+} = 2a + \frac{(-2+(2+(-2+\alpha)\alpha)e^{\alpha})(2-2a)}{\alpha+(-1+\alpha)\alpha e^{\alpha}} \quad (56)$$

The limit of α to zero gives the trapping range of Θ reported in Mishra M and Rao AR (2004) correspond to constant viscosity and if $H_1 = -H_2$ and α approaches zero, we have the results reported by Shapiro *et al.* (1969). For representing the variation of the trapping region, we have chosen $a = b = \omega$ and $d = 1$. For more than one viscosity parameter, Figure-22 shows the trapping region lower limit $\frac{\Theta^{+}}{\Theta_{max}}$ versus ω for three values of ϕ ($\phi = 0, \frac{\pi}{2}$, $\phi = \frac{3\pi}{4}$). It is similar to the constant viscosity case, the region of trapping is decreasing as the phase difference ϕ and similar to the symmetric case, the trapping region for the bivariate viscosity function decreases as the viscosity parameter α and it is smaller than that for a zero viscosity parameter. In Figure-23, the closed streamlines of trapping are plotted for different values of the parameter α and it is clear to note that the trapping seize decreases as α increases.

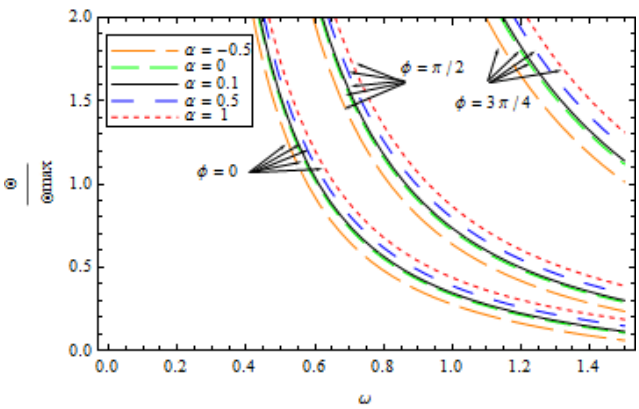

Figure-22. The lower limit of trapping region with various values of viscosity parameter α.

3.3. Reflux limit

The reflux phenomenon is appeared when a fluid particles move backward, on the average. Since the fixed coordinates are considered ideal for the study of the reflux phenomenon, we define the flow-rate function Ψ at x and t, is given by

$$\Psi = \psi + y(\psi, x) - \frac{H_1+H_2}{2} \quad (57)$$

Averaged over one cycle, this becomes

$$\Theta_{\Psi} = \psi + \int_0^1 y(\psi, x)dx - \frac{1+d}{2} \quad (58)$$

In order to evaluate the reflux limit, Θ_{Ψ} is expanded in power series in terms of a small parameter ϵ about the wall, where $\epsilon = \psi - \frac{Q}{2}$ and it is subjected to the reflux condition

$$\frac{\Theta_{\Psi}}{\Theta} > 1 \quad as \quad \epsilon \to 0 \quad (59)$$

The coefficients of the first two terms in the expansion of y, i.e.,

$$y = H_1 + a_0\epsilon + a_1\epsilon^2 + \cdots \quad (60)$$

are found by using (37), as given below

$$a_0 = -1, \quad a_1 = -\frac{\alpha^3 e^{\alpha}(Q+(H1-H_2))}{\beta(H_1-H_2)^2} \quad (61)$$

Using (28), (58), (60) and (61) it follows:

$$\Theta_{\Psi} = \frac{\Theta}{2} - \frac{\alpha^3 e^{\alpha}}{\beta}\frac{(1+d)\Theta-(a^2+b^2+2ab\cos\phi)}{((1+d)^2-(a^2+b^2+2ab\cos\phi))^{\frac{3}{2}}} + \cdots \quad (62)$$

Since $\frac{\alpha^3 e^{\alpha}}{\beta}$ is positive for all $\alpha \neq 0$, and applying the reflux condition (59), the reflux occurs whenever

$$\Theta < \frac{a^2+b^2+2ab\cos\phi}{1+d} \quad (63)$$

is independent to α and is similar to the case of Newtonian fluids with constant viscosity.

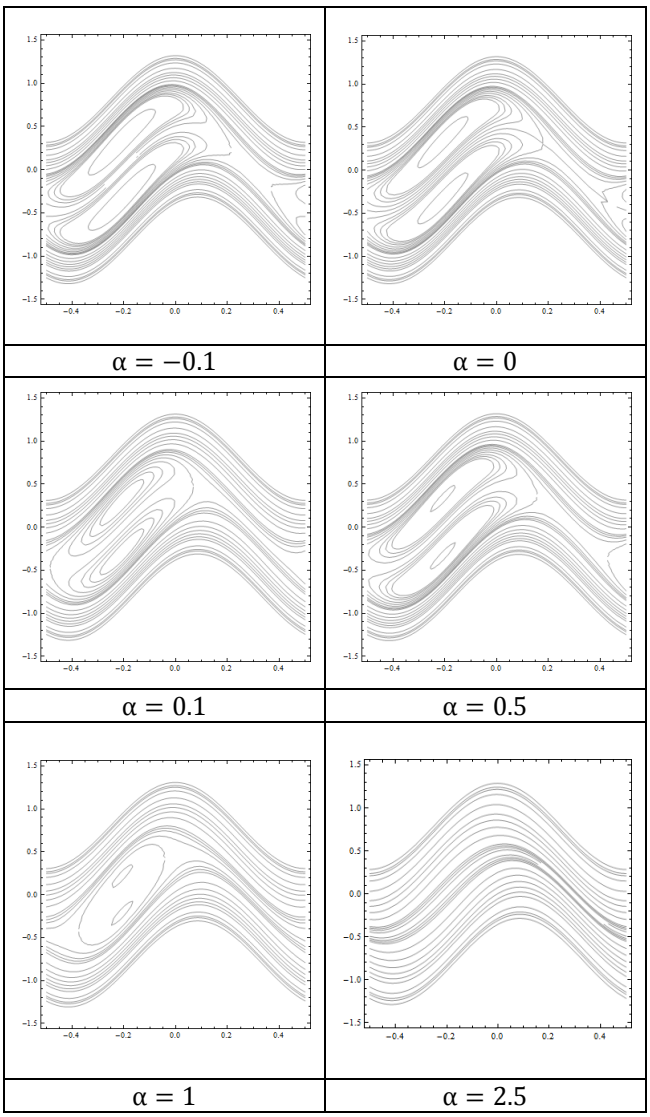

Figure-23. Streamlines in the moved basis for various values of viscosity parameter $\boldsymbol{\alpha}$ and with $\boldsymbol{a = 0.5}$, $\boldsymbol{b = 0.5}$, $\boldsymbol{d = 1}$, $\boldsymbol{\phi = 5\pi/6}$ and $\boldsymbol{\Theta = 1.4}$.

4. CONCLUSIONS

The movement of chyme in small intestine, food bolus through esophagus and the blood in arteries are addressed in this work. Several factors such as viscosity, membranes shape, wave speed and type of fluid, directly affect the pressure, flow and particle velocity. Proper modeling requires the best representation of the factors that gives results that are significantly close to the natural state. For this purpose, a bivariate viscosity function is adapted to analyze the peristaltic motion of a Newtonian fluid in an asymmetric channel. This function was chosen a generalization to that of the case of an axisymmetric conduit such that it is invariant on each proportional membrane surfaces and it is subject to the influence of two different walls at the top and bottom, resulting in a constant viscosity at the midpoints between the two walls. Thus, the stream-lines of viscosity in each half of the channel is influenced by the form of the outer wall and the shape of midpoints locus. We have adopted these notes from some biological studies, which focused on the circulation of the blood and digestive juices and the factors influencing them. It is what makes us believe that the results of this study achieve the reality of some biological phenomena and helps to handle and process multiple body organs in case of malfunction. The results reported by Mishra and Rao (2004) and that reported by Lachiheb (2014) are a special case for this work. The pressure gradient and the friction forces expressions per wavelength are derived. The effects of the upper and lower wave amplitudes, the viscosity function, the channel width and the phase difference on the all flow components are studied. A graphical analysis shows a decrease of the viscosity (increase of the parameter α) reduces the frictional forces on the walls and the pressure rise. Similar to the axisymmetric case, this work also illustrates that, the reflux limit and the free pumping do not depend on the viscosity parameter but the trapping limit, the pressure rise and the friction force on the walls, are influenced by the variation of this parameter. It is observed that the norm of the pressure rise and the friction forces for bivariate viscosity function is less than that reported by Mishra and Rao (2004) for all values of ϕ, a, b and d, while the curve of the pressure rise and the frictional forces for bivariate viscosity function lie under that for one variable viscosity function, for most of values of ϕ, a, b and d. The situation is quite opposite in the pumping region and the region where the friction forces have a direction opposite to that of the wave velocity for some values of ϕ, a, b and d such that ϕ close to π, a to 0.2, b to 0.3 or d to 2. In these latter cases the effect of viscosity is very low. Moreover, the trapping region and size are smaller than to those reported by Mishra and Rao (2004).

ACKNOWLEDGEMENTS

The author gratefully acknowledges the Deanship of Scientific Research at Taibah University on material and moral support in the financing of this research Project.

REFERENCES

[1] Abbasi A, Ahmad I, Ali N, Hayat T. 2016. An analysis of peristaltic motion of compressible convected Maxwell fluid. AIP Advances 6. 015119.

[2] Asha SK and Rathod VP. 2011. Peristaltic transport of a magnetic fluid in a Uniform and Non-Uniform Annulus. IJMA. 12: 1-11.

[3] Brasseur JG, Corrsin S, Lu NQ. 1987. The influence of peripheral layer of different viscosity on peristaltic pumping with Newtonian fluids. J Fluid Mech. 174: 459-519.

[4] Bugliarello G, Sevilla J. 1970. Velocity distribution and other characteristics of steady and pulsatile blood flow in fine glass tubes. Biorheology. 7: 85-107.

[5] Costanzo LS. 2009. Physiology. 4th edition, Elsevier.

[6] Dharmendra T. 2011. A mathematical model for the peristaltic flow of chyme movement in small intestine. Mathematical Biosciences. 233: 90-97.

[7] El Misery AEM, El Naby AH, El Nagar AH. 2003. Effects of a Fluid with Variable Viscosity and an Endoscope on Peristaltic Motion. J Phys Soc Jpn. 72: 89-93.

[8] El Naby AH, El Misiery AEM, El Shamy I. 2003. Hydromagnetic flow of fluid with variable viscosity in a uniform tube with peristalsis. J Phys A: Math Gen. 36: 8535-8547.

[9] El Naby AH, El Misery AEM, El Shamy I. 2004. Effects of an endoscope and fluid with variable viscosity on peristaltic motion. Appl Math Comput. 158: 497-511.

[10] Elshehawey EF, Gharsseldien ZM. 2004. Peristaltic transport of three-layered flow with variable viscosity. Appl Math Comput. 153: 417-432.

[11] Eytan O, Elad D. 1999. Analysis of intra-uterine motion induced by uterine contractions. Bull Math Biol. 61: 221-238.

[12] Gold smith HL, Skalak R. 1975. Hemodynamics, in: M. Van Dyke (Ed). Annual Review of Fluid Mech, vol 7, Annual Review Inc Palo Alto Publ, California. 231-247.

[13] Grobelnik B. 2008. Blood Flow. Postgradute seminar, University in Ljubljana, Faculty of Mathematics and Physics.

[14] Haynes HR. 1960. Physical basis of the dependence of blood viscosity on tube radius. Am J Physiol. 198:1193-1200.

[15] Hayat T, Abbasi FM, Ahmad B, Alsaedi A. 2014. MHD Mixed Convection Peristaltic Flow with Variable Viscosity and Thermal Conductivity. Sains Malaysiana. 43: 1583-1590.

[16] Hayat T, Ali N. 2008. Effect of variable viscosity on the peristaltic transport of a Newtonian fluid in an asymmetric channel. Appl Math Modell. 32: 761-774.

[17] Hina S, Hayat T, Alsaedi A. 2014. Slip Effects on MHD Peristaltic Motion with Heat and Mass Transfer, Arabian J Sci Eng 39:593-603.

[18] Kothandapani M, Prakash J, Pushparaj V. 2016. Nonlinear peristaltic motion of a Johnson– Segalman fluid in a tapered asymmetric channel. AEJ. 55: 1607-1618.

[19] Lucas ML. 2008. Enterocyte chloride and water secretion into the small intestine after enterotoxin challenge: unifying hypothesis or intellectual dead end?. J Physiol Biochem. 64: 69-88.

[20] Lachiheb M. 2014. Effect of coupled radial and axial variability of viscosity on the peristaltic transport of Newtonian Fluid. Appl Math Comput. 244: 761-771.

[21] Lachiheb M. 2016. On the Effect of variable viscosity on the peristaltic transport of a Newtonian fluid in an asymmetric channel, Can J Phys. 94: 320-327.

[22] Latham TW. 1966. Fluid motions in a peristaltic pump. M S Thesis, M I T.

[23] Misra JC, Maiti S. 2012. Peristaltic Transport of a Rheological Fluid: Model for Movement of Food Bolus through Esophagus. J Appl. Math Mech. 33: 315-332.

[24] Mishra M, Rao AR. 2004. Peristaltic transport of a Newtonian fluid in an asymmetric channel. Z Angew Math Phys. 54: 532-550.

[25] Muthu P, Rathish Kumar BV, Chandra P. 2001. Peristaltic motion in circular cylindrical tubes: effect of wall properties. Indian J. pura appl. math. 32: 1317-1328.

[26] Muthu P, Rathish Kumar BV, Chandra P. 2008. Peristaltic motion of micropolar fluid in circular cylindrical tubes: Effect of wall properties, Appl. Math. Modell. 32: 2019-2033.

[27] Rathod VP and Devindrappa L. 2013. Slip effect on peristaltic transport of a porous medium in an asymmetric vertical channel by Adomian decomposition method. IJMA. 4: 133-141.

[28] Shapiro AH, Jaffrin MY, Weinberg SL. 1969. Peristaltic pumping with long wavelengths at low Reynolds number. J Fluid Mech. 37: 799-825.

[29] Sher Akbar N. 2015a. Influence of magnetic field on peristaltic flow of a Casson fluid in an asymmetric channel: Application in crude oil refinement. J Magn Magn Mater. 378: 320-326.

[30] Sher Akbar N. 2015b. Natural convective MHD peristaltic flow of a nanofluid with convective surface boundary conditions. J Comput Theor Nanosci. 12: 257-262.

[31] Sher Akbar N. 2015c. Entropy generation and energy conversion rate for the peristaltic flow in a tube with magnetic field. Energy. 82: 23-30.

[32] Sher Akbar N. 2015d. Entropy Generation Analysis for a CNT Suspension Nanofluid in Plumb Ducts with Peristalsis. Entropy. 17: 1411-1424.

[33] Sher Akbar N. 2015e. Application of Eyring-Powell fluid model in peristalsis with nano particles. J Comput Theor Nanosci. 12: 94-100.

[34] Sher Akbar N. 2015f. Heat transfer and carbon nano tubes analysis for the peristaltic flow in a diverging tube. Meccanica. 50: 39-47.

[35] Shukla JB, Parihar RS, Rao BRP, Gupta SP. 1980. Effects of peripheral layer viscosity on peristaltic transport of a bio-fluid. J Fluid Mech. 97: 225-237.

[36] Srivastava LM, Srivastava VP, Sinha SN. 1983a. Peristaltic transport of a physiological fluid Part-I Flow in non-uniform geometry. Biorheology. 20: 153-66.

[37] Srivastava LM, Srivastava VP, Sinha SN. 1983b. Peristaltic transport of a physiological fluid Part-II Flow in uniform geometry. Biorheology. 20: 167-178.

[38] Turvill JL, Farthing MJ. 1999. Water and electrolyte absorption and secretion in the small intestine. Curr Opin Gastroenterol. 15: 108-120.